The influence of the norbornene anchor group in Rumediated ring-opening metathesis polymerization:

# Synthesis of bottlebrush polymers

Samantha J. Scannelli, Mohammed Alaboalirat, Diego Troya, and John B. Matson\*

Department of Chemistry and Macromolecules Innovation Institute, Virginia Tech, Blacksburg,

VA 24061, United States

\*Correspondence: jbmatson@vt.edu

KEYWORDS: Grafting-through, Propagation, Block copolymer, Size exclusion chromatography, Automated chromatography

For Table of Contents use only

# **ABSTRACT**

Ring-opening metathesis polymerization (ROMP) mediated by Grubbs' third-generation catalyst [G3, (H<sub>2</sub>IMes)(Cl)<sub>2</sub>(pyr)<sub>2</sub>RuCHPh] is widely used to make bottlebrush polymers by polymerization of a macromonomer (MM), typically a low molecular weight polymer

functionalized with a norbornene. Termed the grafting-through method, this strategy requires a high degree of living character ("livingness") to form well-defined bottlebrush polymers. Here we studied how various anchor groups, the series of atoms connecting the polymerizable norbornene unit to the polymer side-chain, affect livingness in ROMP in a series of exo-norbornene polystyrene MMs. First, we calculated the HOMO and HOMO/LUMO gap energies of MM structures containing five different anchor groups using density functional theory methods, finding that these energies spanned a range of 10 kcal/mol. We then performed kinetics experiments on each MM with target backbone degrees of polymerization ( $N_{bb}$ ) of 100 to measure the propagation rate constant  $(k_{p,obs})$  under identical conditions. A positive correlation between the HOMO energy and measured  $k_{p,obs}$  values emerged, revealing a 7-fold variation in  $k_{p,obs}$  values across the five MMs, suggesting different degrees of livingness among the anchor groups. A series of studies targeting  $N_{\rm bb}$  values ranging from 100 to 2000 further highlighted these differences: The MMs with high  $k_{p,obs}$  values reached higher conversions at high target  $N_{bb}$  values with lower dispersities (D) than the MMs with lower  $k_{p,obs}$  values. Finally, we evaluated the synthesis of bottlebrush pentablock copolymers using the MMs at the two extremes by injecting an MM aliquot into a catalyst solution five consecutive times, allowing for polymerization of each block before the next injection. MM conversion at each step was higher, and the D values for each block were lower, for the MM with the highest  $k_p$  anchor group compared to the lowest  $k_p$  anchor group. Taken together, these studies highlight how the anchor group dramatically affects both  $k_p$  and livingness in ROMP, which is crucial for the synthesis of precise bottlebrush (co)polymers.

#### INTRODUCTION

Complex synthetic polymer architectures (topologies) have garnered interest over the years due to their ability to capture intricate properties found in nature. A particularly interesting one is bottlebrush polymers, which contain polymer backbones with densely grafted polymeric sidechains, similar to the topology of proteoglycans. 1-5 The densely packed side-chains prevent entanglement of these macromolecules, influencing properties such as elasticity and domain size in solid state materials, and nanoscopic size and shape in solution.<sup>5-10</sup> As a result, bottlebrush polymers have many potential applications including as elastomers with unusual properties, <sup>11-16</sup> as carriers in biomedicine/drug delivery, <sup>17-19</sup> and as photonic crystals, <sup>20-22</sup> and semiconductors. <sup>23-27</sup> Tuning properties in these materials is achieved through adjusting the backbone and side-chain degree of polymerization ( $N_{bb}$  and  $N_{sc}$ , respectively), as well as grafting density (z, the fraction of monomer units that contain side-chains). However, control over these structural features of the resulting polymers is sometimes lost at high  $N_{bb}$  or  $N_{sc}$ , especially when z is near 1. Therefore, living polymerizations are vital for the synthesis of bottlebrush polymers as they allow for control over molecular weight, molecular weight distribution, and retention of chain end functionalities on the side-chains and backbone. 28-29

Living polymerizations are chain polymerizations that lack chain termination and irreversible chain transfer, and in most cases, a fast initiation process enables them to maintain a constant number of kinetic-chain carriers throughout the polymerization.<sup>30</sup> Historically, anionic polymerization was preferred for synthesizing bottlebrush polymers,<sup>31-33</sup> although they were simply referred to as densely grafted polymers until the mid-1990s.<sup>34</sup> More recently, many other polymerization methods that exhibit living characteristics (i.e., "livingness") have been used to synthesize either the backbones or side-chains of bottlebrush polymers, such as atom-transfer

radical polymerization (ATRP) and reversible addition-fragmentation chain transfer (RAFT) polymerization. Since Bowden's seminal work in 2004, ring-opening metathesis polymerization (ROMP) is also commonly used due to its high propagation rates ( $k_p$ ), high functional group tolerance, and relative insensitivity to air and water. Mediated by a transition metal catalyst such as Grubbs' third-generation catalyst [G3, (H<sub>2</sub>IMes)(Cl)<sub>2</sub>(pyr)<sub>2</sub>RuCHPh], ROMP typically has high propagation rates and even higher initiation rates, enabling living characteristics. Low termination rates ( $k_t$ ) are also critical in polymerizations with a high degree of living character, where livingness is defined as  $k_p/k_t$ . In the context of ROMP, termination occurs primarily through catalyst decomposition, with a rate that is generally low, making it a well-suited method for the synthesis of complex architectures such as bottlebrush polymers.

In most cases, ROMP enables the synthesis of well-defined bottlebrush polymers via the polymerization of norbornene-functionalized macromonomers (MMs).<sup>8-9</sup> The collective synthesis of MMs followed by ROMP is referred to as the grafting-through technique, and it enables control over  $N_{sc}$  and  $N_{bb}$ , with the capacity for perfect grafting density (z = 1).<sup>41</sup> However, despite the popularity of ROMP for making complex polymer topologies, bottlebrush polymers prepared by ROMP grafting-through tend to be fairly small due to the loss of living character when polymerizing even moderately sized MMs ( $N_{sc} = 50$ –100) to moderate degrees of polymerization ( $N_{bb} = 100$ –200). This is because  $k_p$  is lower in MMs than in small molecule monomers.<sup>42-44</sup> It is worth noting that this phenomenon is not limited to ROMP—Sheiko and coworkers recently described similar rate decreases between monomers and MMs in ATRP.<sup>45</sup> In contrast to  $k_p$ ,  $k_t$  in ROMP is unlikely to be affected by the length of MM side-chains because it is a function of catalyst decomposition, which primarily (although not entirely) occurs through an intramolecular C–H activation pathway that does not depend heavily on monomer type.<sup>46-47</sup> Therefore, while ATRP

and RAFT achieve high livingness (as quantified by high  $k_p/k_t$  ratios)<sup>48</sup> by reducing  $k_t$ , this option is not available in ROMP using G3 catalyst. Instead, one needs to enhance  $k_p$  to increase livingness in ROMP.

In 2016 we enhanced the  $k_p$  of ROMP mediated by G3 catalyst by tuning MM reactivity.<sup>49</sup> In a recent paper, we presented a thorough investigation of this phenomenon through a combined computational and experimental approach, measuring propagation and termination rates of small molecule monomers in the synthesis of linear polymers.<sup>50</sup> In this recent work, we monitored the polymerization of eight different monomers mediated by G3 catalyst as well as the less active Grubbs 1st generation catalyst [G1, (PCy<sub>3</sub>)<sub>2</sub>(Cl)<sub>2</sub>RuCHPh]. The monomers had varying anchor groups, which is the series of atoms directly connected to the polymerizable unit used in ROMP (norbornene here).<sup>51</sup> We found that the anchor group influenced the energy of the HOMO localized on the norbornene olefin and that an increasing HOMO energy increased  $k_p$  but did not substantially affect  $k_t$ . However, when using the highly active G3 catalyst, the effect on  $k_p$  reached a plateau for the three monomers with the highest HOMO energies, where  $k_p$  remained flat despite a continued increase in the HOMO energy. Interestingly, when using G1 catalyst, where  $k_p$  values were 10–20-fold lower than in G3 catalyst, we saw larger variations in  $k_{\rm p}$  for the three monomers that plateaued in rate with G3 catalyst. Therefore, we hypothesized that adding a side-chain (i.e., using an MM instead of a small molecule norbornene) would slow down polymerization enough for the HOMO energy to influence  $k_p$  in MMs with these three anchor groups. In other words, we envisioned that adding a side-chain would allow us to observe differences among these "fast" (i.e., high  $k_p$ ) anchor groups that were unobservable in small molecule norbornenes.

Here we focus on the ROMP of MMs, quantitatively investigating how the anchor group affects  $k_p$  and livingness in the synthesis of bottlebrush polymers (Scheme 1). We set out to study

five anchor groups of interest, specifically those suitable for attaching a polymer chain to the norbornene as well as easily comparable to equivalent structures in our recent paper.<sup>50</sup> Through the use of computational methods to determine HOMO energy values and experimental methods to measure  $k_p$  values, we investigated the effects of the anchor group in ROMP of MMs. Additionally, we aimed to study how  $k_p$  affects livingness in ROMP by monitoring MM conversion and maximum obtainable bottlebrush polymer  $N_{bb}$  at high [MM]/[G3] ratios (up to 2000). We also anticipated that livingness could be assessed by synthesizing bottlebrush pentablock copolymers in a sequential addition of MMs approach by following molecular weight evolution and increases in dispersity (D) upon the addition of each new block. Overall, we envisioned that these studies could reveal how the anchor group can be tuned to yield maximum (macro)monomer conversion and livingness when synthesizing complex polymer topologies by ROMP.

**Scheme 1.** Representative scheme of grafting-through ROMP of norbornene MMs with various anchor groups where  $n = N_{sc}$  and  $m = N_{bb}$ 

## RESULTS AND DISCUSSION

In the recent paper mentioned in the introduction, we calculated the HOMO and HOMO/LUMO gap energies of 61 monomers with different anchor groups for the synthesis of linear polymers via ROMP.<sup>50</sup> All HOMOs were centered on the norbornene alkene, which interacts with the Ru center in the rate-determining metallacyclobutane formation step in ROMP.<sup>52</sup> Of these 61 monomers, we selected eight anchor groups to synthesize and study experimentally with the goal of identifying the effects of the anchor group on  $k_p$  and livingness in ROMP. Here we focus

on five of these eight anchor groups, including the three that showed the highest  $k_p$  in the ROMP of small molecule norbornenes, in the form of MMs to investigate the effects of the anchor group on livingness in bottlebrush polymer synthesis.

# HOMO Energy Calculations

We first calculated the HOMO energies of the five selected anchor groups attached to a polystyrene (PS) side-chain (MMs 1–5) (Figure 1A). In these computational studies, only one styrene repeat unit, representing the PS side-chain, was used to calculate the molecular orbital energies because we aimed to investigate the HOMO localized on the reactive olefin, which should not be influenced by the side-chain beyond the first repeat unit. The HOMO energies were calculated from optimized geometries of the five monomer structures using density functional theory (DFT) (M06-2X method and def2-TZVP basis set).<sup>53-54</sup> Coordinates of the five monomer structures and the HOMO energies are shown in the Supporting Information. Our goal was to investigate the  $\pi$  bonding orbital of the olefin, as these electrons are involved in the ratedetermining step of norbornenyl ROMP, which corresponds formation of the metallocyclobutane intermediate from the olefin and metal carbene.<sup>52</sup> In MMs x-MOM<sub>2</sub>E'-PS (1) and x-ME'-PS (2), the  $\pi$  bonding orbital was the absolute HOMO (HOMO-0), but in some monomers, this orbital did not correspond to the absolute HOMO. For the anchor group in MM x-EM<sub>2</sub>E'-PS (3), the olefin-centered HOMO was HOMO-1, for MMs xx-IMEM<sub>2</sub>E'-PS (4) and  $xx-IM_2E'-PS$  (5), it was HOMO-2. For the sake of simplicity, we use the term HOMO to refer to "olefin-centered HOMO" in the rest of this paper.

The HOMOs localized on the reactive olefins span energies in the -197 to -187 kcal/mol range, similar to analogous small molecule structures in our related paper.<sup>50</sup> In this related paper,<sup>50</sup>

we also calculated the HOMO/LUMO energy gap for each monomer based on the concept that multiple orbital interactions occur during the formation of the metallocyclobutane ring, as suggested by Suresh and Koha. Here, we hypothesized that MMs with higher norbornene HOMO energies and lower LUMO olefin energies would exhibit faster polymerization rates ( $k_p$  values) and higher livingness in general, as measured in maximum obtainable  $N_{bb}$  studies and bottlebrush pentablock copolymer chain extension studies.

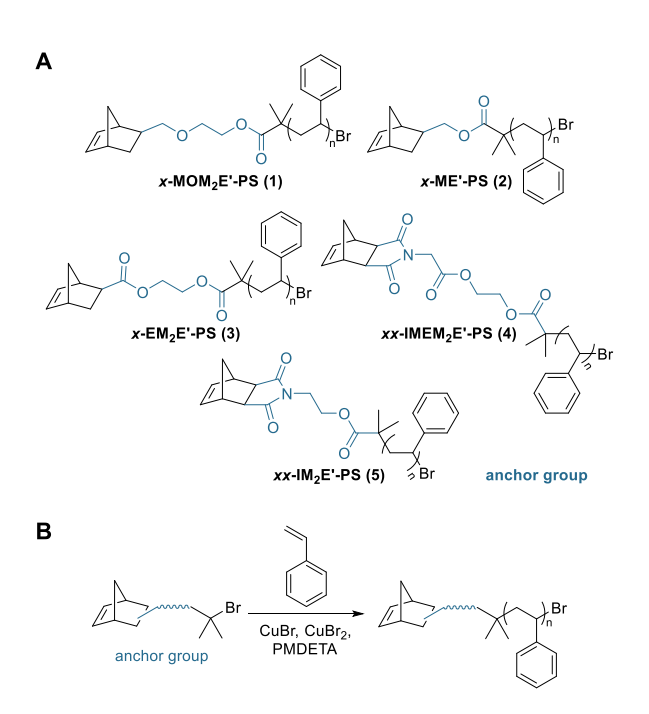


**Figure 1**. (A) Norbornene MMs with various anchor groups (blue) computationally and experimentally investigated where  $n = N_{sc}$ . For computations,  $N_{sc} = 1$  and the Br end group was replaced with H; for experiments,  $N_{sc} = 24-28$ . All monomers exhibited *exo* (x prefix) or *exo-exo* (xx prefix) stereochemistry. Letters identify structural components of the anchor group from left to right (M = methylene, O = oxygen, E = ester with carbonyl on the left, E' = ester with carbonyl on the right, I = imide); all MM side-chains are polystyrene (PS). Subscripts indicate the number of times that component is repeated. (B) Representative synthesis of PS MMs via ATRP. Polymerizations were conducted at 90 °C for 3 h targeting 10% conversion of styrene.

We employed ATRP to synthesize five PS MMs (Figure 1B), all with number-average molecular weight values ( $M_n$ ) near 3 kg/mol. We designed these MMs to have the same polymer side-chain and  $M_n$  to isolate the contributions of the anchor group on  $k_p$ . Each was synthesized using the direct-growth approach from five different norbornene-derived initiators (Table 1). Standard conditions of Cu(I)Br, Cu(II)Br, and  $N_iN_iN_iN_iN_iN_i$ -pentamethyldiethylenetriamine (PMDETA) were used in all cases and polymerizations were conducted at 90 °C for 3 h. We targeted 10% monomer conversion in the ATRP reactions to avoid termination by coupling, which would result in MMs with norbornene groups on both chain ends. <sup>56</sup>

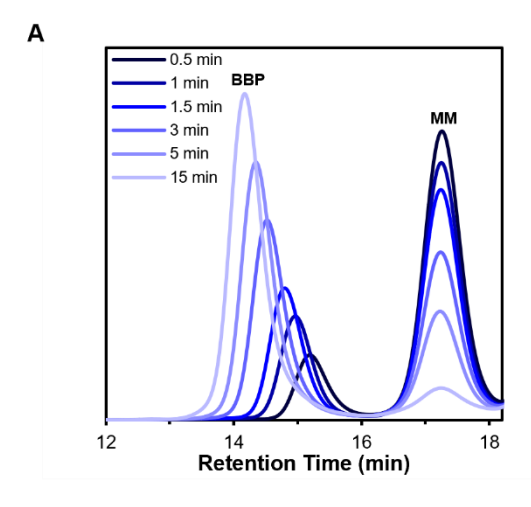
Because any residual impurities, in particular styrene monomer but also Cu catalyst or ligand, could detrimentally affect the rate of ROMP, 57-59 we extensively purified each MM. In brief, crude MMs were diluted with water and extracted with ethyl acetate to remove Cu species, then purified by automated silica gel chromatography using an ethyl acetate/hexane gradient as the mobile phase. After solvent removal, each MM was passed through basic alumina in tetrahydrofuran (THF), and finally precipitated into methanol. Automated flash chromatography, which monitors UV absorbance throughout the separation (Figures S15–S19), provided confidence in the removal of all residual monomer through the clear separation between the styrene peak that elutes first and the broad MM peak that elutes later, as we showed previously. <sup>56</sup> Passage of the polymer solution through an alumina plug after column purification presumably removed trace catalyst and/or ligand that remained; we observed lower conversion to bottlebrush polymer when this step was not carried out. A final precipitation step into methanol afforded the final MM products as white powders, making them easy to work with for the subsequent ROMP step.

**Table 1.** Characterization of PS MMs

MM	$M_{ m n,SEC}^{a}$	$M_{ m n,NMR}^{b}$	$\mathcal{D}^a$	
IVIIVI	(kg/mol)	(kg/mol)	$D^{\circ}$	
<i>x</i> -MOM <sub>2</sub> E'-PS (1)	3.2	2.9	1.06	
<i>x</i> -ME'-PS ( <b>2</b> )	3.2	3.3	1.08	
x-EM <sub>2</sub> E'-PS (3)	2.9	3.2	1.07	
xx-IMEM <sub>2</sub> E'-PS (4)	2.9	3.3	1.09	
xx-IM <sub>2</sub> E'-PS (5)	2.9	3.4	1.06	

<sup>a</sup>Measured by SEC in THF at 30 °C with multiangle light scattering. <sup>b</sup>Measured by end-group analysis via <sup>1</sup>H NMR spectroscopy. See Figures S20–S29.

Each MM was next polymerized via ROMP to investigate the differences in  $k_{\rm p,obs}$  based on the anchor group. Polymerizations of all MMs were mediated by G3 catalyst with a targeted  $N_{\rm bb}$  of 100 at a concentration of 20 mM in CDCl<sub>3</sub>, under air and at room temperature. Aliquots were removed and terminated with an excess of ethyl vinyl ether at predetermined time intervals, the solvent was removed, and each aliquot was then analyzed by size exclusion chromatography (SEC). MM conversion at each time point was measured by comparing the areas of the MM peak and bottlebrush polymer peak. Average  $k_{\rm p,obs}$  values and half-lives were calculated from first-order kinetics plots for at least three polymerizations per MM. The conversion versus time data and first-order fits are shown in Figure 2 for a representative MM, x-MOM<sub>2</sub>E'-PS (1). Similar graphs for the other four MMs are included in the Supporting Information (Figures S30–S39).



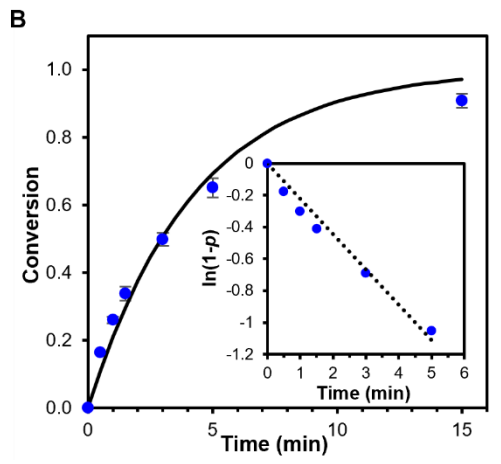


**Figure 2**. (A) Representative SEC traces (dRI signal) of the ROMP of MM x-MOM<sub>2</sub>E'-PS (1) at an [MM]/[G3] ratio of 100:1. As the polymerization proceeds, the MM signal at 17.2 min decreases in intensity and the bottlebrush polymer signal increases in intensity and shifts in retention time from 15.2 min to 14 min. (B) Kinetic analysis of the ROMP of MM x-MOM<sub>2</sub>E'-PS (1) in CDCl<sub>3</sub> at an [MM]/[G3] ratio of 100:1 and [MM] = 20 mM. The solid line represents the fit to the averaged conversion data based on the equation  $p = 1 - e^{(-k_{obs}t)}$  where p = fractional conversion.

As expected, each MM polymerized slower, by approximately an order of magnitude, compared with analogue small molecule monomer structures, <sup>50</sup> where the only difference lies in the presence of the PS side-chain. MM x-ME'-PS (2) had the highest  $k_{p,obs}$  out of all the MMs tested and polymerized 7-fold faster than the MM with the lowest  $k_{p,obs}$  [xx-IM<sub>2</sub>E'-PS (5)]. MMs 1–3 all had half-lives under 4 min, whereas the imide-based MMs (4–5) had half-lives over 13 min. Relatively low dispersities and good agreement between expected and measured  $M_n$  values

for the resulting bottlebrush polymers suggest high livingness in all of these polymerizations (Table 2).

**Table 2**. HOMO energies, HOMO/LUMO gap energies, polymerization kinetics, and bottlebrush polymer characterization for ROMP of MMs 1–5

polyther characterization for ROWI of Wilvis 1–3								
	HOMO	HOMO/				BB	BB	
MM	Energy <sup>a</sup> (kcal/mol)	LUMO Gap (kcal/mol) <sup>a</sup>	$k_{p,obs}^{b}$ (min <sup>-1</sup> )	t <sub>1/2</sub> (min)	% conv <sup>c</sup>	$M_{ m n,expected}^d$ (kg/mol)	$M_{ m n,SEC}^e$ (kg/mol)	BB
x-MOM <sub>2</sub> E'-PS (1)	-187	214	$0.23 \pm 0.02$	$3.0 \pm 0.2$	98	320	325	1.06
<i>x</i> -ME'-PS ( <b>2</b> )	-187	214	$0.31\pm0.03$	$2.3 \pm 0.2$	98	320	295	1.04
x-EM <sub>2</sub> E'-PS (3)	-191	211	$0.19 \pm 0.01$	$3.7 \pm 0.1$	98	290	296	1.05
xx-IMEM <sub>2</sub> E'-PS (4)	-196	217	$0.052\pm0.01$	$13.4\pm0.3$	98	290	251	1.07
xx-IM <sub>2</sub> E'-PS (5)	-197	218	$0.040 \pm 0.003$	$17 \pm 1$	98	290	302	1.07

<sup>a</sup>Calculated using M06-2X method and def2-TZVP basis set. <sup>53-54</sup> <sup>b</sup>Calculated from conversions measured by SEC on aliquots removed at specific time points during the polymerizations. A minimum of three polymerizations were run for each MM. <sup>c</sup>Measured on the final sample of the kinetics runs using SEC by comparing the areas of the bottlebrush polymer and MM peaks in the dRI trace. <sup>d</sup>Determined using the equation  $M_{n,\text{expected}} = M_{n,\text{MM}} * ([\text{MM}]/[\text{G3}])_0$ . <sup>e</sup>Measured on the final sample of the kinetics runs by SEC in THF at 30 °C with multiangle light scattering using the known dn/dc for PS of 0.185 mL/g.

We next examined how HOMO energy influenced  $k_p$ . By plotting the HOMO energies calculated for the MMs versus the experimentally measured  $k_{p,obs}$  values, we found a positive correlation between HOMO energy and  $k_{p,obs}$  for these five MMs (Figure 3). We found an inverse correlation for the HOMO/LUMO energy gaps and the  $k_{p,obs}$  values for each MM (Figure S40). Evidently, multiple orbital interactions are important during the rate-determining step, but we focus here on the HOMO energy as a simple predictor for relative  $k_p$  values. Both trends were similar to the eight different anchor groups in analogous molecule monomers, 50 with MMs x-MOM<sub>2</sub>E'-PS (1), x-ME'-PS (2), and x-EM<sub>2</sub>E'-PS (3) with the highest HOMO energies exhibiting the highest  $k_{p,obs}$  values and the MMs xx-IMEM<sub>2</sub>E'-PS (4) and xx-IM<sub>2</sub>E'-PS (5) with

lower HOMO energies undergoing slower polymerization. In the small molecule norbornene monomers, there were no measurable differences in  $k_{\rm p,obs}$  among monomers polymerized using G3 catalyst with anchor groups similar to those in MMs 1–3.<sup>50</sup> In this MM study, however,  $k_{\rm p,obs}$  values were different among these three anchor groups. Interestingly, MM x-ME'-PS (2) showed the highest  $k_{\rm p,obs}$  value even though MM x-MOM<sub>2</sub>E'-PS (1) had a slightly higher HOMO energy, although the 0.8 kcal/mol difference between these two MMs is likely within the accuracy of the methods used.

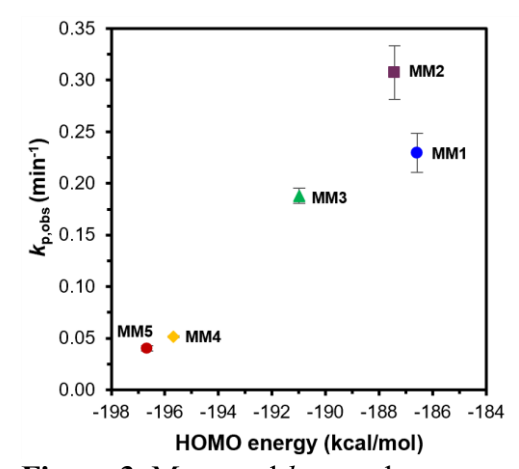


**Figure 3**. Measured  $k_{p,obs}$  values versus HOMO energy for MMs 1–5.

Effects of the Anchor Group on Livingness in High Target N<sub>bb</sub> Bottlebrush Polymers

Polymerizations that exhibit living characteristics have high  $k_p/k_t$  ratios, enabling the synthesis of polymers with high degrees of polymerization while maintaining low D values. High livingness in ROMP grafting-through of MMs is critical for the synthesis of precise bottlebrush polymers. Control over  $M_n$  and D of the resulting bottlebrush polymers can be lost when targeting high  $N_{bb}$  values due to the increased number of required successful catalyst turnovers compared to polymerizations targeting low  $N_{bb}$  values. Therefore, as a method of evaluating livingness, we

designed a series of experiments examining grafting-through ROMP with high [MM]/[G3] ratios (i.e., target  $N_{bb}$  values ranging from 100 to 2000). By comparing the experimentally observed  $N_{bb}$  values (as estimated by the equation  $N_{bb} = M_{n,bottlebrush}/M_{n,MM}$ ) to their target  $N_{bb}$  values across the five MMs studied here, we envisioned that this set of experiments would reveal the most living anchor groups, i.e., those with the highest  $k_p/k_t$  ratios. We hypothesized that MM x-ME'-PS (2), which had the highest  $k_p$ , would exhibit the highest livingness in these experiments because anchor group choice did not substantially affect  $k_t$  in small molecule norbornenes.<sup>50</sup>

The high target  $N_{bb}$  experiments were prepared at an MM concentration of 20 mM in CDCl<sub>3</sub>, under air and at room temperature, similar to the kinetics experiments described above. We set the target  $N_{bb}$  (i.e., [MM]/[G3] ratio) to 100, 250, 500, 750, 1000, 1500, and 2000 for each of the MMs. Each ROMP reaction was terminated after 24 h with an excess of ethyl vinyl ether to ensure maximum conversion was reached. The solvent was removed and the residual polymer was redissolved in THF for SEC analysis. All polymerizations were run at least three times.

MM conversion versus target  $N_{bb}$  (Figure 4A) and measured  $N_{bb}$  versus target  $N_{bb}$  (Figure 4B) were plotted for all five MMs (error bars were not included in the graphs for the sake of clarity and are provided in Tables S1–S5). All MMs reached high conversion (>90%) and showed measured  $N_{bb}$  values matching target values when with an [MM]/[G3] ratio of 100:1, similar to the kinetics experiments. However, even at a modest [MM]/[G3] ratio of 250:1, MMs xx-IMEM<sub>2</sub>E'-PS (4) and xx-IM<sub>2</sub>E'-PS (5) failed to exceed 90% conversion and did not reach target  $N_{bb}$  values. These two MMs showed even lower conversion (<60%) and significant deviation from targeted  $N_{bb}$  with  $D \sim 1.4$  at an [MM]/[G3] ratio of 500:1. Less than 3% MM conversion was observed for MM xx-IM<sub>2</sub>E'-PS (5) at target  $N_{bb} = 1000$  and higher, and MM xx-IMEM<sub>2</sub>E'-PS (4) barely polymerized to form bottlebrush polymer at or above target  $N_{bb} = 1500$ . Thus, these two imide-

based anchor groups only exhibited a high degree of livingness up to  $N_{bb} = 100$ , consistent with the lower livingness for imide-based anchor groups in small molecule norbornenes.<sup>50</sup>

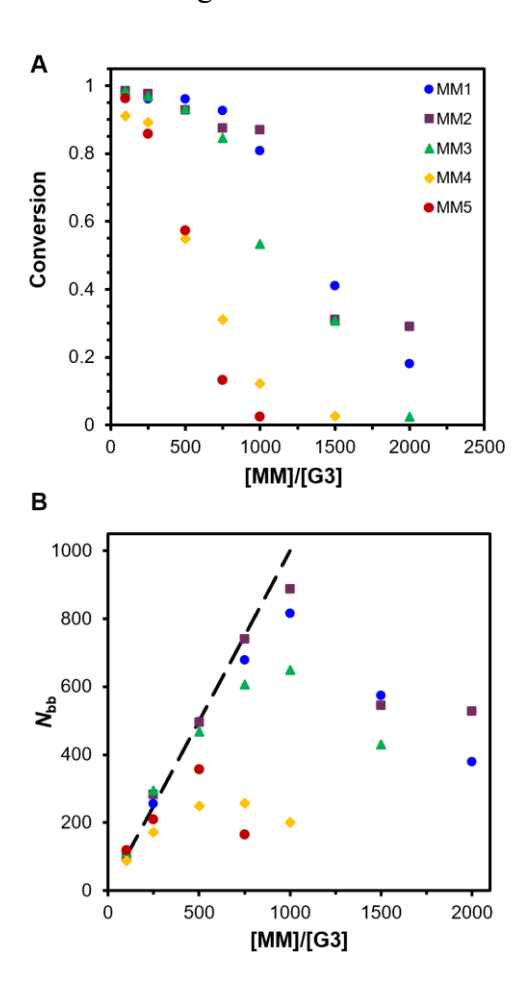


**Figure 4.** (A) Fractional MM conversion to bottlebrush polymer after 24 h versus target  $N_{\rm bb}$  values, referred to as [MM]/[G3] ratio, for grafting-through ROMP of the five MMs studied here. Reactions were conducted at 20 mM in MM in CDCl<sub>3</sub> under air at rt. Conversion was measured using SEC by comparing the areas of the bottlebrush polymer and MM peaks in the dRI trace. (B) Measured  $N_{\rm bb}$  versus target  $N_{\rm bb}$  values, referred to as [MM]/[G3] ratio. The black dashed line refers to expected  $N_{\rm bb}$  as [MM]/[G3] increases. Measured  $N_{\rm bb}$  values were determined from  $M_{\rm n,bottlebrush}$  obtained by SEC in THF at 30 °C with multiangle light scattering, calculated based on the equation  $N_{\rm bb} = M_{\rm n,bottlebrush}/M_{\rm n,MM}$ . In both graphs, error bars were removed for better visualization of the data but can be found in Tables S1–S5.

The three MMs with higher  $k_p$  values (1–3) showed high livingness out to higher target  $N_{bb}$  values than MMs xx-IMEM<sub>2</sub>E'-PS (4) and xx-IM<sub>2</sub>E'-PS (5). MM x-EM<sub>2</sub>E'-PS (3) showed >90% conversion and  $N_{bb}$  matching expected values out to a target  $N_{bb} = 500$ , but experienced lower

conversion and large deviations from target  $N_{bb}$  values at 750 and higher, with <3% conversion to bottlebrush polymer observed at  $N_{bb} = 2000$ . MMs x-MOM<sub>2</sub>E'-PS (1) and x-ME'-PS (2), those with the highest  $k_{p,obs}$  and HOMO energies, maintained high conversion (>90%) up to an [MM]/[G3] ratio of 500:1 with D values <1.2. They both reached very good conversion (>80%) with  $N_{bb}$  matching expected values out to a target  $N_{bb} = 1000$ , although D values increased to 1.5–1.6. A substantial drop in conversion when targeting  $N_{bb} = 1500$  and higher was observed for both MMs, but some conversion was still observed even at target  $N_{bb} = 2000$ . Therefore, MMs x-MOM<sub>2</sub>E'-PS (1) and x-ME'-PS (2) maintained the most livingness of all five MMs during the grafting-through ROMP process with the highest MM conversion, best control over  $M_n$  (i.e., experimentally observed  $N_{bb}$ ), and lowest D values out all the MMs investigated.

It is worth noting that MM x-ME'-PS (2) had the highest conversion and highest observed  $N_{bb}$  when targeting  $N_{bb} = 2000$  out of MMs 1–5, even though it was not highly living at this high target  $N_{bb}$ . These results, combined with the  $k_{p,obs}$  results (Table 2), suggest that the anchor group in MM x-ME'-PS (2) was the most living anchor group studied here. In contrast, MM xx-IM<sub>2</sub>E'-PS (5) had the lowest  $k_{p,obs}$  and performed the worst in the high target  $N_{bb}$  studies, making MM xx-IM<sub>2</sub>E'-PS (5) the least living anchor group out of the five MMs tested. Therefore, we decided to further compare the livingness of these two MMs in chain extension studies using the sequential addition of macromonomers ROMP (SAM-ROMP) process.

Effects of the Anchor Group on Livingness in Bottlebrush Pentablock Copolymer Synthesis

Multiblock bottlebrush copolymers with three or more blocks have been recently used to make electronic materials,<sup>60</sup> injectable hydrogels,<sup>61-62</sup> solid electrolytes,<sup>63</sup> and nanostructures with unusual shapes.<sup>64-65</sup> High livingness in block copolymer synthesis is critical for complete chain

extension, so in order to evaluate the effect of the anchor group on chain extension, we conducted a series of studies on the synthesis of bottlebrush pseudo-pentablock copolymers. In these SAM-ROMP studies, we aimed to follow evolution of molecular weight and D over the course of five consecutive additions of the same MM with a target  $N_{bb} = 20$  for each addition. This strategy of consecutive additions of the same MM allowed us to remove any potential variable reactivity of different MMs, but we expect that the results would be useful in making complex structures with up to five different MMs.

The first step was to determine the time required for each MM to reach near-complete conversion (>95%) at a target  $N_{bb} = 20$ ; therefore, we conducted kinetics experiments for MM x-ME'-PS (2) and xx-IM<sub>2</sub>E'-PS (5) with an [MM]/[G3] ratio of 20:1. Polymerizations were carried out and monitored under the same conditions and using the same methods as the other polymerizations described here. In these experiments, MM x-ME'-PS (2) had a propagation half-life of 1.4 min and MM xx-IM<sub>2</sub>E'-PS (5) had a propagation half-life of 13.4 min, with both MMs reaching near-complete conversion based on SEC analysis at very close to 7 half-lives [10 min for MM x-ME'-PS (2) and 90 min for MM xx-IM<sub>2</sub>E'-PS (5)].

We then set out to compare bottlebrush pentablock copolymer synthesis for the two MMs. The pentablock polymerizations via the SAM-ROMP method were conducted under the same conditions as described above, injecting 20 equiv of the same MM five times at intervals of either 10 min [MM x-ME'-PS (2)] or 90 min [MM xx-IM<sub>2</sub>E'-PS (5)] (Figure 5A and 5E). Aliquots were removed right before each MM injection to determine conversion,  $M_n$ , and D of each block (Table 3).

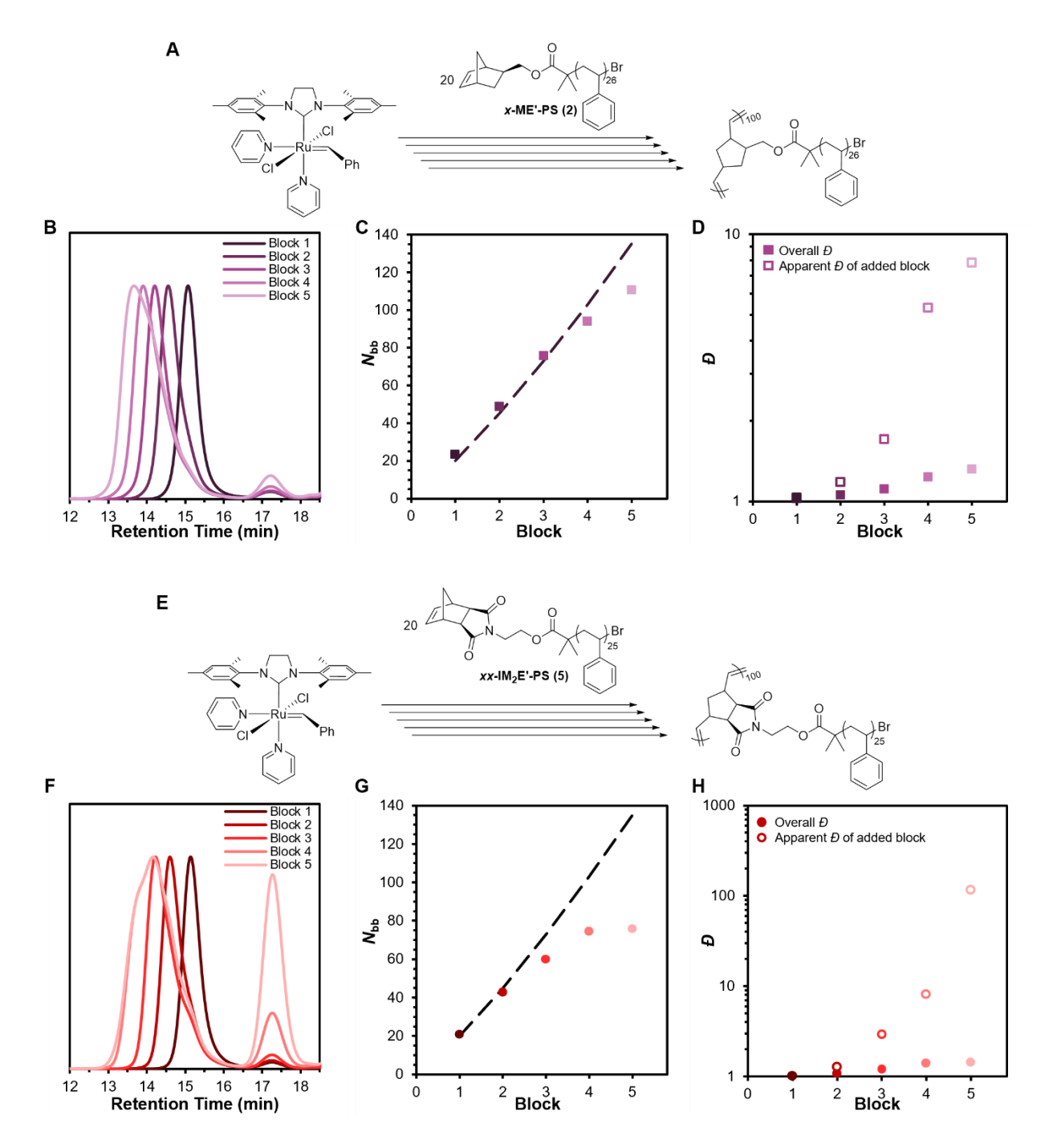


**Figure 5.** A and E): Schemes for bottlebrush pentablock copolymer syntheses for the ROMP of MMs x-ME'-PS (2) (A) and xx-IM<sub>2</sub>E'-PS (5) (E). Reactions were run at a total MM concentration of 20 mM in CDCl<sub>3</sub> under air at rt. B and F): SEC traces (dRI signal) for the ROMP of MM x-ME'-PS (2) (B) and xx-IM<sub>2</sub>E'-PS (5) (F) showing a decrease in retention time after each block addition. C and G): Measured  $N_{bb}$  value versus block number for the ROMP of MM x-ME'-PS (2) (C) and xx-IM<sub>2</sub>E'-PS (5) (G). Measured  $N_{bb}$  values were determined from  $M_{n,bottlebrush}$  measured by SEC in THF at 30 °C with multiangle light scattering, estimated based on the equation  $N_{bb} = M_{n,bottlebrush}/M_{n,MM}$ . The dashed line refers to expected  $N_{bb}$  as block number increases. D and H): Overall D and apparent D of each added block for the ROMP of MM x-ME'-PS (2) (D) and

xx-IM<sub>2</sub>E'-PS (**5**) (H). Apparent D refers to the estimated dispersity of each specific block as calculated by the method developed by Harrisson using the formula  $D_2 = 1 + \frac{\mu_{1+2}^2(D_{1+2}-1) - \mu_1^2(D_1-1)}{(\mu_{1+2}-\mu_1)^2}$  where  $D_2$  is the apparent dispersity in terms of the number-average molar masses of the initial ( $\mu_1$ ) and final ( $\mu_{1+2}$ ) polymers and the overall dispersity of the initial ( $\mu_1$ ) and final ( $\mu_1$ ) polymers.<sup>66</sup>

Table 3. Characterization of Bottlebrush Pentablock Copolymers Prepared by SAM-ROMP

204	Block	%	BB $M_{n,expected}^b$	$BB M_{n,SEC}^c$	Total	Total	BB	Apparent
MM	#	conv <sup>a</sup>	(kg/mol)	(kg/mol)	Target N <sub>bb</sub>	$N_{ m bb,  SEC}^d$	$\mathcal{D}^{c}$	$D^e$
<i>x</i> -ME'-PS (2)	1	97	64	70	20	23	1.03	1.03
	2	97	128	147	40	48	1.06	1.18
	3	97	192	227	60	76	1.11	1.71
	4	96	256	282	80	94	1.23	5.3
	5	95	320	332	100	110	1.32	7.8
xx-IM <sub>2</sub> E'-PS ( <b>5</b> )	1	97	58	60	20	21	1.02	1.02
	2	97	116	124	40	43	1.08	1.27
	3	96	174	174	60	60	1.20	2.9
	4	89	232	216	80	74	1.40	8.1
	5	71	290	220	100	75	1.43	116

<sup>a</sup>Measured using SEC by comparing the areas of the bottlebrush polymer and MM peaks in the dRI trace. <sup>b</sup>Determined using the equation  $M_{n,expected} = M_{n,MM} * ([MM]/[G3])_0$ . <sup>c</sup>Measured by SEC in THF at 30 °C with multiangle light scattering using the known dn/dc for PS of 0.185 mL/g. <sup>d</sup>Determined using the equation  $N_{bb,expected} = M_{n,bottlebrush}/M_{n,MM}$ . <sup>e</sup>Determined using the method developed by Harrisson. <sup>66</sup>

For both MM x-ME'-PS (2) and MM xx-IM<sub>2</sub>E'-PS (5), we saw a decrease in the retention time of the main SEC peak upon polymerization of each additional block, indicating an increase in molecular weight of the bottlebrush polymer (Figures 5B and 5F). As expected, the first block for both MMs reached near-complete conversion (>97%) while maintaining low D. However, MM conversion generally decreased after each block addition, with MM x-ME'-PS (2) dropping to 95% conversion and MM xx-IM<sub>2</sub>E'-PS (5) dropping to just 71% conversion after the addition of all five

blocks. A small residual MM peak at 17.2 min was observed in the final SEC trace for the ROMP of MM x-ME'-PS (2), while a much more prominent MM peak remained for MM xx-IM<sub>2</sub>E'-PS (5).

We also observed an increase in  $N_{bb}$  after each block addition, as determined by SEC, for both MMs, as expected (Figure 5C and 5G). After each injection of MM x-ME'-PS (2), a linear increase in  $N_{bb}$  was observed. All  $N_{bb}$  values generally matched target values for this MM as well, with a final estimated  $N_{bb} = 110$  for the bottlebrush pentablock copolymer, close to the target  $N_{bb}$  value of 100. The small deviations from the expected values are likely due to small errors in injected monomer amount or catalyst loading. In contrast, this close agreement between target  $N_{bb}$  and measured  $N_{bb}$  values was not the case for the bottlebrush polymer derived from MM xx-IM<sub>2</sub>E'-PS (5). A linear increase in  $N_{bb}$  matching target values was found for the first three MM injections, but blocks 4 and 5 did not reach target  $N_{bb}$  values. For this imide-based anchor group, we observed a maximum  $N_{bb} = 75$ , where only very little polymerization was observed for the fifth MM injection.

Comparing the bottlebrush polymer D values and the shapes of the SEC curves after every block addition for both MMs also revealed valuable insights regarding livingness. For the bottlebrush polymer derived from MM x-ME'-PS (2), D values reached 1.3, but they increased to 1.4 for the bottlebrush polymer derived from MM xx-IM<sub>2</sub>E'-PS (5) (Table 3). Furthermore, the bottlebrush polymers with a final target  $N_{bb}$  = 100 for both MMs made by the SAM-ROMP method exhibited higher D values than those synthesized directly to a target  $N_{bb}$  value of 100 (1.04 for MM x-ME'-PS (2) and 1.07 for MM xx-IM<sub>2</sub>E'-PS (5), from the kinetics data in Table 2). Additionally, low molecular weight shoulders were present in the SEC traces for blocks 4 and 5 for the ROMP of MM x-ME'-PS (2) and blocks 3 through 5 for the ROMP of MM xx-IM<sub>2</sub>E'-PS

(5), suggesting some amount of chain termination in both ROMP experiments before all five blocks had been added. However, the shoulders in the SEC traces of the bottlebrush polymers derived from MM xx-IM<sub>2</sub>E'-PS (5) were drastically larger than in those derived from MM x-ME'-PS (2), clearly indicating a lower degree of livingness for MM xx-IM<sub>2</sub>E'-PS (5) compared with MM x-ME'-PS (2). This reduced livingness for MM xx-IM<sub>2</sub>E'-PS (5) was not as readily apparent in the high target  $N_{bb}$  studies, where this MM reached a total  $N_{bb}$  of 100, matching the target  $N_{bb}$  value, with high conversion and low D; however, these SAM-ROMP studies make clear that the relatively low  $k_{p,obs}$  for MM xx-IM<sub>2</sub>E'-PS (5) leads to low livingness when challenging the catalyst with multiple MM injections.

Only a small difference in D values (1.3 versus 1.4) between the final polymers in these two SAM-ROMP experiments was found, but we were interested in estimating the D values of each individual bottlebrush polymer block in these pentablock copolymers. Harrisson recently reported a mathematical method of estimating the apparent D of each individual block in a linear multiblock copolymer synthesis. <sup>66</sup> His results in a study of a 24-block copolymer made by RAFT <sup>67</sup> suggested that the individual substructures of complex macromolecules may be highly disperse even though the overall D remains relatively low. Using this method, we estimated the apparent D of each individual block in both bottlebrush pentablock copolymer syntheses (Figure 5D and 5H). For both MMs, the apparent D of each block increased roughly exponentially, consistent with Harrisson's analysis, but with very different outcomes between the two SAM-ROMP experiments: The final block of MM x-ME'-PS (2) reached an apparent D of 7.8, whereas the final block of MM x-IM<sub>2</sub>E'-PS (5) had an apparent D of 116. This order of magnitude difference between the two anchor groups dramatically demonstrates the higher degree of livingness for MM x-ME'-PS (2) compared with MM x-IM<sub>2</sub>E'-PS (5). The data also suggest that even with MM x-ME'-PS (2), the

most living anchor group studied here, there is still significant chain termination when making bottlebrush pentablock copolymers. Overall, we conclude that high  $k_p$  is critical in the ROMP of MMs to control molecular weight, maintain low dispersity, and retain high chain end fidelity when synthesizing multiblock bottlebrush copolymers, but that even for the best anchor group studied here, structural heterogeneities arise.

#### CONCLUSIONS

We investigated the relationship between HOMO energies localized on the norbornene olefin and livingness in the ROMP of a series of five MMs with PS side-chains of similar molecular weights but different anchor groups. DFT calculations showed that the choice of anchor group affects the norbornene HOMO energy of these MMs, and experimental results suggested that a higher HOMO energy increases the reactivity of the norbornene and increases  $k_p$  in graftingthrough ROMP. Further investigation into the livingness of grafting-through ROMP through high target  $N_{bb}$  studies demonstrated that high  $k_p$  values are critical to synthesize macromolecules with precise molecular weights and low D values. MMs with lower HOMO energies (those with imidecontaining anchor groups), and lower  $k_{p,obs}$  values in our ROMP experiments, showed lower livingness at target  $N_{\rm bb} = 250$  and above than the other MMs. However, the two MMs with the highest HOMO energies and  $k_{p,obs}$  values reached high conversion and maintained control over molecular weight when targeting  $N_{\rm bb}$  values up to 1000. Therefore, MMs with anchor groups that lead to higher  $k_p$  values increase livingness in grafting-through ROMP compared with MMs with lower  $k_p$  values, allowing for better-defined bottlebrush polymer structures. The effect of the anchor group on livingness was further evidenced in SAM-ROMP experiments synthesizing bottlebrush pentablock copolymers using the MMs with the highest and lowest  $k_{p,obs}$  values (MMs

x-ME'-PS (2) and xx-IM<sub>2</sub>E'-PS (5), respectively). Each block addition of MM xx-IM<sub>2</sub>E'-PS (5)

exhibited an increase in the D value of both the overall polymer structure and the apparent D of

each additional block, where the final block had a staggering apparent D of 116. A similar effect

was seen for the SAM-ROMP of MM x-ME'-PS (2) to make a bottlebrush pentablock copolymer;

however, the increase in apparent D was significantly lower, only reaching 7.8 for the final block.

In sum, these experiments indicate that high  $k_p$  values in ROMP are critical to maintain

high livingness for the synthesis of complex macromolecules such as bottlebrush polymers, and

that anchor group selection has a substantial effect on  $k_p$ . Our studies were designed to evaluate

the effect of the anchor group on  $k_p$  in a defined set of MMs of similar molecular weights, but we

expect that these results will suggest straightforward methods to enhance livingness and control in

a wide variety of polymer topologies made by ROMP. These experiments also underscore the need

to develop better anchor groups that increase  $k_p$  and better catalysts that decrease  $k_t$  in ROMP, as

well as improved methods that increase the  $k_p/k_t$  ratio, to continue to expand the synthetic

boundaries of complex polymer architectures.

ASSOCIATED CONTENT

**Supporting Information** 

Supporting Information: Synthesis, NMR spectra, kinetics graphs, SEC traces, HOMO energies,

and coordinates (PDF)

## **AUTHOR INFORMATION**

# **Corresponding Author**

John B. Matson – Department of Chemistry and Macromolecules Innovation Institute, Virginia Tech, Blacksburg 24061 Virginia, United States

#### **Author Contributions**

Samantha J. Scannelli – Department of Chemistry and Macromolecules Innovation Institute, Virginia Tech, Blacksburg 24061 Virginia, United States

Mohammed Alaboalirat – Department of Chemistry and Macromolecules Innovation Institute,

Virginia Tech, Blacksburg 24061 Virginia, United States

Current address: Research and Development Center, Saudi Aramco, Dhahran 31311, Saudi Arabia

Diego Troya – Department of Chemistry and Macromolecules Innovation Institute, Virginia Tech, Blacksburg 24061 Virginia, United States

## **Notes**

The authors declare no competing financial interest.

## **ACKNOWLEDGMENTS**

This work was supported by a joint grant between the National Science Foundation and the Binational Science Foundation (DMR-2104602). We thank Dr. Santu Sarkar, Tamalika Paul, and Ishani Sarkar for critical reading of the manuscript. The authors acknowledge Advanced Research Computing at Virginia Tech for providing computational resources and technical support that have contributed to the results reported within this paper. We also acknowledge the Virginia Tech Mass Spectrometry Research Incubator for high-resolution mass spectrometry analysis.

#### REFERENCES

- 1. Jha, S.; Dutta, S.; Bowden, N. B., Synthesis of Ultralarge Molecular Weight Bottlebrush Polymers Using Grubbs' Catalysts. *Macromolecules* **2004**, *37*, 4365-4374.
- 2. Wintermantel, M.; Gerle, M.; Fischer, K.; Schmidt, M.; Wataoka, I.; Urakawa, H.; Kajiwara, K.; Tsukahara, Y., Molecular Bottlebrushes. *Macromolecules* **1996**, *29*, 978-983.
- 3. Xie, G.; Martinez, M. R.; Olszewski, M.; Sheiko, S. S.; Matyjaszewski, K., Molecular Bottlebrushes as Novel Materials. *Biomacromolecules* **2019**, *20*, 27-54.
- 4. Li, Z.; Tang, M.; Liang, S.; Zhang, M.; Biesold, G. M.; He, Y.; Hao, S.-M.; Choi, W.; Liu, Y.; Peng, J.; Lin, Z., Bottlebrush polymers: From controlled synthesis, self-assembly, properties to applications. *Prog. Polym. Sci.* **2021**, *116*, 101387.
- 5. Sheiko, S. S.; Sumerlin, B. S.; Matyjaszewski, K., Cylindrical molecular brushes: Synthesis, characterization, and properties. *Prog. Polym. Sci.* **2008**, *33*, 759-785.
- 6. Verduzco, R.; Li, X.; Pesek, S. L.; Stein, G. E., Structure, function, self-assembly, and applications of bottlebrush copolymers. *Chem. Soc. Rev.* **2015**, *44*, 2405-2420.
- 7. Zhulina, E. B.; Sheiko, S. S.; Borisov, O. V., Theoretical advances in molecular bottlebrushes and comblike (co)polymers: solutions, gels, and self-assembly. *Soft Matter* **2022**, *18*, 8714-8732.
- 8. Walsh, D. J.; Guironnet, D., Macromolecules with programmable shape, size, and chemistry. *Proc. Natl. Acad. Sci. U.S.A* **2019**, *116*, 1538-1542.
- 9. Dearman, M.; Ogbonna, N. D.; Amofa, C. A.; Peters, A. J.; Lawrence, J., Versatile strategies to tailor the glass transition temperatures of bottlebrush polymers. *Polym. Chem.* **2022**, *13*, 4901-4907.
- 10. Kamble, Y. L.; Walsh, D. J.; Guironnet, D., Precision of Architecture-Controlled Bottlebrush Polymer Synthesis: A Monte Carlo Analysis. *Macromolecules* **2022**, *55*, 10255-10263.
- 11. Maw, M.; Morgan, B. J.; Dashtimoghadam, E.; Tian, Y.; Bersenev, E. A.; Maryasevskaya, A. V.; Ivanov, D. A.; Matyjaszewski, K.; Dobrynin, A. V.; Sheiko, S. S., Brush Architecture and Network Elasticity: Path to the Design of Mechanically Diverse Elastomers. *Macromolecules* **2022**, *55*, 2940-2951.
- 12. Self, J. L.; Sample, C. S.; Levi, A. E.; Li, K.; Xie, R.; de Alaniz, J. R.; Bates, C. M., Dynamic Bottlebrush Polymer Networks: Self-Healing in Super-Soft Materials. *J. Am. Chem. Soc.* **2020**, *142*, 7567-7573.
- 13. Sarapas, J. M.; Chan, E. P.; Rettner, E. M.; Beers, K. L., Compressing and Swelling To Study the Structure of Extremely Soft Bottlebrush Networks Prepared by ROMP. *Macromolecules* **2018**, *51*, 2359-2366.
- 14. Cushman, K.; Keith, A.; Tanaka, J.; Sheiko, S. S.; You, W., Investigating the Stress–Strain Behavior in Ring-Opening Metathesis Polymerization-Based Brush Elastomers. *Macromolecules* **2021**, *54*, 8365-8371.
- 15. Arrington, K. J.; Radzinski, S. C.; Drummey, K. J.; Long, T. E.; Matson, J. B., Reversibly Cross-linkable Bottlebrush Polymers as Pressure-Sensitive Adhesives. *ACS Appl. Mater. Interfaces* **2018**, *10*, 26662-26668.

- 16. Neary, W. J.; Fultz, B. A.; Kennemur, J. G., Well-Defined and Precision-Grafted Bottlebrush Polypentenamers from Variable Temperature ROMP and ATRP. *ACS Macro Lett.* **2018**, *7*, 1080-1086.
- 17. Ramamurthi, P.; Zhao, Z.; Burke, E.; Steinmetz, N. F.; Müllner, M., Tuning the Hydrophilic–Hydrophobic Balance of Molecular Polymer Bottlebrushes Enhances their Tumor Homing Properties. *Adv. Healthc. Mater.* **2022**, *11*, 2200163.
- 18. Nguyen, H. V. T.; Jiang, Y.; Mohapatra, S.; Wang, W.; Barnes, J. C.; Oldenhuis, N. J.; Chen, K. K.; Axelrod, S.; Huang, Z.; Chen, Q.; Golder, M. R.; Young, K.; Suvlu, D.; Shen, Y.; Willard, A. P.; Hore, M. J. A.; Gómez-Bombarelli, R.; Johnson, J. A., Bottlebrush polymers with flexible enantiomeric side chains display differential biological properties. *Nat. Chem.* **2022**, *14*, 85-93.
- 19. Sowers, M. A.; McCombs, J. R.; Wang, Y.; Paletta, J. T.; Morton, S. W.; Dreaden, E. C.; Boska, M. D.; Ottaviani, M. F.; Hammond, P. T.; Rajca, A.; Johnson, J. A., Redox-responsive branched-bottlebrush polymers for in vivo MRI and fluorescence imaging. *Nat. Commun.* **2014**, *5*, 5460.
- 20. Miyake, G. M.; Piunova, V. A.; Weitekamp, R. A.; Grubbs, R. H., Precisely Tunable Photonic Crystals From Rapidly Self-Assembling Brush Block Copolymer Blends. *Angew. Chem* **2012**, *51*, 11246-11248.
- 21. Liberman-Martin, A. L.; Chang, A. B.; Chu, C. K.; Siddique, R. H.; Lee, B.; Grubbs, R. H., Processing Effects on the Self-Assembly of Brush Block Polymer Photonic Crystals. *ACS Macro Lett.* **2021**, *10*, 1480-1486.
- 22. Boyle, B. M.; French, T. A.; Pearson, R. M.; McCarthy, B. G.; Miyake, G. M., Structural Color for Additive Manufacturing: 3D-Printed Photonic Crystals from Block Copolymers. *ACS Nano* **2017**, *11*, 3052-3058.
- 23. van As, D.; Subbiah, J.; Jones, D. J.; Wong, W. W. H., Controlled Synthesis of Well-Defined Semiconducting Brush Polymers. *Marcomol. Chem. Phys.* **2016**, *217*, 403-413.
- 24. Tonge, C. M.; Sauvé, E. R.; Cheng, S.; Howard, T. A.; Hudson, Z. M., Multiblock Bottlebrush Nanofibers from Organic Electronic Materials. *J. Am. Chem. Soc.* **2018**, *140*, 11599-11603.
- 25. Sauvé, E. R.; Tonge, C. M.; Hudson, Z. M., Aggregation-Induced Energy Transfer in Color-Tunable Multiblock Bottlebrush Nanofibers. *J. Am. Chem. Soc.* **2019**, *141*, 16422-16431.
- 26. Obhi, N. K.; Peda, D. M.; Kynaston, E. L.; Seferos, D. S., Exploring the Graft-To Synthesis of All-Conjugated Comb Copolymers Using Azide–Alkyne Click Chemistry. *Macromolecules* **2018**, *51*, 2969-2978.
- 27. Pelras, T.; Nonappa; Mahon, C. S.; Müllner, M., Cylindrical Zwitterionic Particles via Interpolyelectrolyte Complexation on Molecular Polymer Brushes. *Macromol. Rapid Commun.* **2021**, *42*, 2000401.
- 28. Szwarc, M., Living polymers. Their discovery, characterization, and properties. *J. Polym. Sci., Part A: Polym. Chem.* **1998**, *36*, IX-XV.
- 29. Stenzel, M. H.; Barner-Kowollik, C., The living dead common misconceptions about reversible deactivation radical polymerization. *Mater. Horiz.* **2016**, *3*, 471-477.
- 30. Jenkins, A. D.; Kratochvíl, P.; Stepto, R. F. T.; Suter, U. W., Glossary of basic terms in polymer science (IUPAC Recommendations 1996). *Pure Appl. Chem.* **1996**, *68*, 2287-2311.
- 31. Desimone, J. M.; Hellstern, A. M.; Siochi, E. J.; Smith, S. D.; Ward, T. C.; McGrath, J. E.; Gallagher, P. M.; Krukonis, V. J., Homogeneous and multiphase poly(methyl methacrylate) graft polymers via the macromonomer method. *Makromol. Chem. Macromol. Symp.* **1990**, *32*, 21-45.

- 32. Rahlwes, D.; Roovers, J. E. L.; Bywater, S., Synthesis and Characterization of Poly(styrene-g-isoprene) Copolymers. *Macromolecules* **1977**, *10*, 604-609.
- 33. Hadjichristidis, N.; Iatrou, H.; Pitsikalis, M.; Mays, J., Macromolecular architectures by living and controlled/living polymerizations. *Prog. Polym. Sci.* **2006**, *31*, 1068-1132.
- 34. Wintermantel, M.; Fischer, K.; Gerle, M.; Ries, R.; Schmidt, M.; Kajiwara, K.; Urakawa, H.; Wataoka, I., Lyotropic Phases Formed by "Molecular Bottlebrushes". *Angew. Chem., Int. Ed. Engl.* **1995**, *34*, 1472-1474.
- 35. Matyjaszewski, K., Atom Transfer Radical Polymerization: From Mechanisms to Applications. *Isr. J. Chem.* **2012**, *52*, 206-220.
- 36. Keddie, D. J.; Moad, G.; Rizzardo, E.; Thang, S. H., RAFT Agent Design and Synthesis. *Macromolecules* **2012**, *45*, 5321-5342.
- 37. Cheng, C.; Khoshdel, E.; Wooley, K. L., ATRP from a Norbornenyl-Functionalized Initiator: Balancing of Complementary Reactivity for the Preparation of α-Norbornenyl Macromonomers/ω-Haloalkyl Macroinitiators. *Macromolecules* **2005**, *38*, 9455-9465.
- 38. Bielawski, C. W.; Grubbs, R. H., Living ring-opening metathesis polymerization. *Prog. Polym. Sci.* **2007**, *32*, 1-29.
- 39. Choi, T.-L.; Grubbs, R. H., Controlled Living Ring-Opening-Metathesis Polymerization by a Fast-Initiating Ruthenium Catalyst. *Angew. Chem* **2003**, *42*, 1743-1746.
- 40. Trnka, T. M.; Grubbs, R. H., The Development of L2X2RuCHR Olefin Metathesis Catalysts: An Organometallic Success Story. *Acc. Chem. Res.* **2001**, *34*, 18-29.
- 41. Blosch, S. E.; Scannelli, S. J.; Alaboalirat, M.; Matson, J. B., Complex Polymer Architectures Using Ring-Opening Metathesis Polymerization: Synthesis, Applications, and Practical Considerations. *Macromolecules* **2022**, *55*, 4200-4227.
- 42. Ren, N.; Yu, C.; Zhu, X., Topological Effect on Macromonomer Polymerization. *Macromolecules* **2021**, *54*, 6101-6108.
- 43. Ogbonna, N. D.; Dearman, M.; Cho, C.-T.; Bharti, B.; Peters, A. J.; Lawrence, J., Topologically Precise and Discrete Bottlebrush Polymers: Synthesis, Characterization, and Structure–Property Relationships. *JACS Au* **2022**, *2*, 898-905.
- 44. Walsh, D. J.; Guironnet, D., Macromolecules with programmable shape, size, and chemistry. *Proc. Natl. Acad. Sci.* **2019**, *116*, 1538-1542.
- 45. Cong, Y.; Vatankhah-Varnosfaderani, M.; Karimkhani, V.; Keith, A. N.; Leibfarth, F. A.; Martinez, M. R.; Matyjaszewski, K.; Sheiko, S. S., Understanding the Synthesis of Linear–Bottlebrush–Linear Block Copolymers: Toward Plastomers with Well-Defined Mechanical Properties. *Macromolecules* **2020**, *53*, 8324-8332.
- 46. Hong, S. H.; Wenzel, A. G.; Salguero, T. T.; Day, M. W.; Grubbs, R. H., Decomposition of Ruthenium Olefin Metathesis Catalysts. *J. Am. Chem. Soc.* **2007**, *129*, 7961-7968.
- 47. Bailey, G. A.; Foscato, M.; Higman, C. S.; Day, C. S.; Jensen, V. R.; Fogg, D. E., Bimolecular Coupling as a Vector for Decomposition of Fast-Initiating Olefin Metathesis Catalysts. *J. Am. Chem. Soc.* **2018**, *140*, 6931-6944.
- 48. Matyjaszewski, K., Ranking living systems. *Macromolecules* **1993**, *26*, 1787-1788.
- 49. Radzinski, S. C.; Foster, J. C.; Chapleski, R. C.; Troya, D.; Matson, J. B., Bottlebrush Polymer Synthesis by Ring-Opening Metathesis Polymerization: The Significance of the Anchor Group. *J. Am. Chem. Soc.* **2016**, *138*, 6998-7004.
- 50. Scannelli, S. J.; Paripati, A.; Weaver, J. R.; Alaboalirat, M.; Troya, D.; Matson, J. B., The influence of the anchor group in ring-opening metathesis polymerization: Synthesis of linear polymers. *Macromolecules* **2023**, *Submitted*, ma-2023-001729.

- 51. Slugovc, C.; Demel, S.; Riegler, S.; Hobisch, J.; Stelzer, F., The Resting State Makes the Difference: The Influence of the Anchor Group in the ROMP of Norbornene Derivatives. *Macromol. Rapid Commun.* **2004**, *25*, 475-480.
- 52. Hyatt, M. G.; Walsh, D. J.; Lord, R. L.; Andino Martinez, J. G.; Guironnet, D., Mechanistic and Kinetic Studies of the Ring Opening Metathesis Polymerization of Norbornenyl Monomers by a Grubbs Third Generation Catalyst. *J. Am. Chem. Soc.* **2019**, *141*, 17918-17925.
- 53. Zhao, Y.; Truhlar, D. G., The M06 suite of density functionals for main group thermochemistry, thermochemical kinetics, noncovalent interactions, excited states, and transition elements: two new functionals and systematic testing of four M06-class functionals and 12 other functionals. *Theor. Chem. Acc*, **2008**, *120*, 215-241.
- 54. Weigend, F.; Ahlrichs, R., Balanced basis sets of split valence, triple zeta valence and quadruple zeta valence quality for H to Rn: Design and assessment of accuracy. *Phys. Chem. Phys.* **2005**, *7*, 3297-3305.
- 55. Suresh, C. H.; Koga, N., Orbital Interactions in the Ruthenium Olefin Metathesis Catalysts. *Organometallics* **2004**, *23*, 76-80.
- 56. Alaboalirat, M.; Vu, C.; Matson, J. B., Radical–radical coupling effects in the direct-growth grafting-through synthesis of bottlebrush polymers using RAFT and ROMP. *Polym. Chem.* **2022**, *13*, 5841-5851.
- 57. Lexer, C.; Saf, R.; Slugovc, C., Acrylates as termination reagent for the preparation of semi-telechelic polymers made by ring opening metathesis polymerization. *J. Polym. Sci., Part A: Polym. Chem.* **2009**, *47*, 299-305.
- 58. Choi, J.; Kim, H.; Do, T.; Moon, J.; Choe, Y.; Kim, J. G.; Bang, J., Influence of residual impurities on ring-opening metathesis polymerization after copper(I)-catalyzed alkyne-azide cycloaddition click reaction. *J. Polym. Sci., Part A: Polym. Chem.* **2019**, *57*, 726-737.
- 59. Teo, Y. C.; Xia, Y., Importance of Macromonomer Quality in the Ring-Opening Metathesis Polymerization of Macromonomers. *Macromolecules* **2015**, *48*, 5656-5662.
- 60. Polgar, A. M.; Poisson, J.; Christopherson, C. J.; Hudson, Z. M., Enhancement of Red Thermally Assisted Fluorescence in Bottlebrush Block Copolymers. *Macromolecules* **2021**, *54*, 7880-7889.
- 61. Nakagawa, Y.; Oki, Y.; Da, X.; Singh Chandel, A. K.; Ohta, S.; Ito, T., Injectable bottlebrush triblock copolymer hydrogel crosslinked with ferric ions. *Polymer* **2022**, *240*, 124519.
- 62. Vohidov, F.; Milling, L. E.; Chen, Q.; Zhang, W.; Bhagchandani, S.; Nguyen, Hung V. T.; Irvine, D. J.; Johnson, J. A., ABC triblock bottlebrush copolymer-based injectable hydrogels: design, synthesis, and application to expanding the therapeutic index of cancer immunochemotherapy. *Chem. Sci.* **2020**, *11*, 5974-5986.
- 63. Bates, C. M.; Chang, A. B.; Momčilović, N.; Jones, S. C.; Grubbs, R. H., ABA Triblock Brush Polymers: Synthesis, Self-Assembly, Conductivity, and Rheological Properties. *Macromolecules* **2015**, *48*, 4967-4973.
- 64. Radzinski, S. C.; Foster, J. C.; Scannelli, S. J.; Weaver, J. R.; Arrington, K. J.; Matson, J. B., Tapered Bottlebrush Polymers: Cone-Shaped Nanostructures by Sequential Addition of Macromonomers. *ACS Macro Lett.* **2017**, *6*, 1175-1179.
- 65. Li, A.; Li, Z.; Zhang, S.; Sun, G.; Policarpio, D. M.; Wooley, K. L., Synthesis and Direct Visualization of Dumbbell-Shaped Molecular Brushes. *ACS Macro Lett.* **2012**, *1*, 241-245.
- 66. Harrisson, S., The downside of dispersity: why the standard deviation is a better measure of dispersion in precision polymerization. *Polym. Chem.* **2018**, *9*, 1366-1370.

67. Engelis, N. G.; Anastasaki, A.; Nurumbetov, G.; Truong, N. P.; Nikolaou, V.; Shegiwal, A.; Whittaker, M. R.; Davis, T. P.; Haddleton, D. M., Sequence-controlled methacrylic multiblock copolymers via sulfur-free RAFT emulsion polymerization. *Nat. Chem.* **2017**, *9*, 171-178.